Generalized Test Bed for High-Voltage, High-Power SiC Device Characterization

David Berning, Allen Hefner, Jose M. Ortiz-Rodriguez, Colleen Hood, and Angel Rivera
Semiconductor Electronics Division
National Institute of Standards and Technology, Gaithersburg, MD, 20899 USA

***Abstract*-- A generalized 25 kV test bed developed to characterize high-voltage, high-power SiC devices is described. The test bed provides a high-speed (30 μs), high-voltage linear amplifier that is used as the pulsed power supply for parametric static measurements (curve tracer) and as the continuous high voltage power supply for inductive/resistive switching measurements. The test bed includes high-voltage inductors, clamping capacitors, and load modules for resistive and inductive load switching. An additional reconfigurable section of the test bed with plug-in current limiting and current sense resistors is used for parametric (curve tracer) device characterization. A flexible curve tracer software-based user interface is used to control several power supply and measurement instruments that collectively comprise a versatile pulsed curve tracer. The device under test (DUT) is mounted on a 20 kV electrically-isolated temperature-controlled heatsink. The test bed features containment of all high voltage circuits and the DUT within a clear plastic interlocked safety box. Several example measurements of SiC devices using the test bed are shown.[1]**

Key words: Curve tracer; DUT; high power; high voltage MOSFET; inductive load switching; parametric testing; power conversion; SiC; semiconductor device characterization.

I. INTRODUCTION

Recently, silicon carbide (SiC) power devices have begun to emerge with performance that is superior to that of silicon (Si) power devices. For a given blocking voltage, minority carrier conductivity modulated devices such as PiN diodes made using the SiC material are expected to show an improvement in switching speed by a factor of 100 as compared to Si devices. In addition, majority carrier SiC devices, such as MOSFETs, are expected to show a factor of 100 advantage in having lower resistance compared to that of Si majority carrier devices [1]. The larger bandgap of SiC (3.26 eV for 4H-SiC [1] versus 1.1 eV for Si) also provides the potential for SiC devices to operate at much higher temperatures than their Si counterparts. These advantages in electronic and material properties are driving the development of new high-voltage SiC devices that push the performance envelope of power device technologies [2].

Organizations that have a need for large power systems are driving the development of high-voltage, high-frequency SiC power electronic devices. The Electric Power Research Institute (EPRI) has concluded that a solid-state distribution transformer, referred to as the Intelligent Universal Transformer (IUT), would add significant new functional capabilities to those available from conventional copper and iron transformers. A recent EPRI report concluded that future IUT product generations may migrate to SiC power semiconductors if they become available at suitable ratings [3]. Furthermore, the goal of an ongoing Defense Advanced Research Projects Agency (DARPA) Wide Bandgap Semiconductor Technology High Power Electronics (WBST-HPE) program is to support the research and development necessary to realize the SiC semiconductor components, both a switch and a diode, with the main focus being on power electronics technologies for 10 kV class devices. Applications include power distribution and electro-magnetics weapons in future hybrid-electric combat vehicles, naval ship propulsion, and electric aircraft. [4].

The work presented in this paper addresses the device measurement methods and metrology needed for this new class of SiC power semiconductor devices having combined high-voltage and high-speed switching capability. This paper describes the design and use of a new 25 kV test bed for static parametric and switching characterization of high voltage SiC power semiconductor devices. Several examples are given to demonstrate the features and operation of the new test bed in characterizing high voltage SiC devices.

II. TEST BED HARDWARE COMPONENTS

The high-voltage SiC testing system hardware consists of an array of purchased instruments operated under computer control and a group of custom circuit modules and power sources. The computer-controlled instruments include such items as an oscilloscope for data acquisition, pulse and function generators, temperature controller, and programmable voltage/current sources. The custom electronics include a fast high power amplifier/power supply, a high-speed 25 kV converter module, a high-voltage isolated device heatsink and driver, and modules for device switching measurements and for pulsed I-V parametric measurements. All of the high voltage circuits

[1] Contribution of the National Institute of Standards and Technology, not subject to copyright. The devices shown in this paper were produced by Cree Inc. under the DARPA WBST HPE Phase 2 program sponsored by Sharon Beermann-Curtin and monitored by Harry Dietrich.

and the device under test (DUT) are contained in a safety-interlocked clear plastic box.

The amplifier/power supply, located outside of the box, is a 750 watt linear unipolar power source that supplies power to the DUT through the high voltage converter or directly to the DUT for low voltage, high current measurements. The amplifier can deliver 30 V at 25 A with a 30 µs risetime and has an analog input for applying pulses to the DUT, as well as a knob for manually applying dc voltages to the converter. With this amplifier, the output of the 25 kV converter is limited to approximately 17 kV at 40 mA, but the amplifier can be upgraded to obtain the full 25 kV capability designed into the test bed.

The remainder of this section describes the various custom electronic circuits used for characterizing high-voltage SiC devices for leakage, transfer characteristics, resistive and inductive switching, and ruggedness. Fig. 1 shows the various circuit blocks that are housed in the high-voltage plastic box. The 25 kV converter module, its driver and interlock, and the temperature-controlled heatsink are non-configurable and are built into separate protected areas that are not user accessible. Both the parametric characterization module and the switching module are accessible for configuration of the required measurement.

A. I-V Parametric Characterization Module

The I-V parametric characterization module shown in fig. 1 is used to provide pulsed curve tracer type measurements. This module is used with a custom LabView/CVI[2] application program that is summarized below and more fully described in section III. The heatsink-mounted DUT is connected to the output of the 25 kV converter through a plug-in resistor module shown as R_{LOAD} in the figure. The 25 kV converter output is floating and can be configured for either positive or negative ground. A current sensing resistor R_{SENSE}, also shown in the figure, is chosen by the user to use the full range of the oscilloscope voltage scale. The voltage across R_{SENSE} is applied to one channel of the scope, and is used to by the curve tracer program to calculate the DUT current where the user supplies the value of R_{SENSE} to the program. The use of the current waveform in determining a single current value will be explained in section III.

R_{LOAD} is a current limiting resistor and is selected by the user to safely limit the DUT current as the supply voltage is increased for each measured data point. As an example, suppose a 10 kV leakage test is being performed, and the user wishes to limit the maximum current to 20 µA. The number of data points to be taken is 100, starting at 100 V. This divides the voltage supply sweep into 100 V increments. Let's further suppose that a particular DUT has a very abrupt breakdown characteristic at an unknown voltage within this range, representing a worst case scenario. If the user selects R_{LOAD} to be 10 MΩ, the incremental change in current can be no more than 10 µA. If the user were to set the curve tracer software maximum current to 10 µA, the program will stop the measurement sequence before the current can reach 20 µA. The voltage at the DUT- R_{LOAD} terminal is measured with an appropriate voltage probe and fed to one channel of the scope. This voltage is used by the curve tracer program to calculate the DUT voltage waveform by subtracting the voltage waveform across R_{SENSE}. A single voltage value is obtained from the voltage waveform in a manner similar to that used to obtain the single value for the current waveform as explained in section III.

In the case of a MOSFET parametric measurement, the gate of the DUT is driven with a voltage that is applied between the gate and source terminals. This voltage is stepped as the parametric I-V curves are generated by the software. Protection and noise-filtering devices are applied in the gate and source circuits, but are not shown in the figure. A commercial instrument that is operated under the control of the curve tracer software is used to supply the gate voltage, but this instrument can also be directed to supply current for characterizing bipolar devices.

B. Switching Module

The switching module is placed into use by changing configuration jumpers shown in fig. 1 so that the output from the 25 kV converter is applied to the clamp capacitors, four large 1µF, 15 kV oil capacitors connected in parallel with a low inductance copper planar bus. The amplifier/power supply is now used in the dc mode to drive the 25 kV converter rather than the in linear amplifier mode used for the curve tracer. The user sets the high voltage DUT power supply using the manual knob on the 750 watt low-voltage power supply with the aid of a DVM located

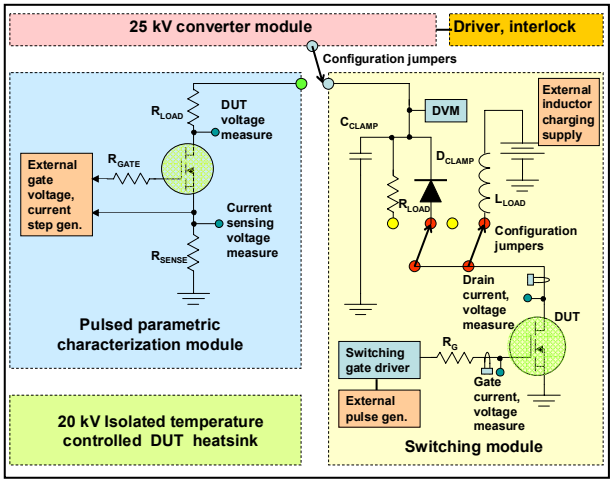

Fig. 1. Diagram of generalized test bed showing the configuration of the various modules.

[2] Certain commercial products are identified to better explain the conducted research. This identification does not imply an endorsement by the National Institute of Standards and Technology, nor does it imply that these products are necessarily the best for the purpose.

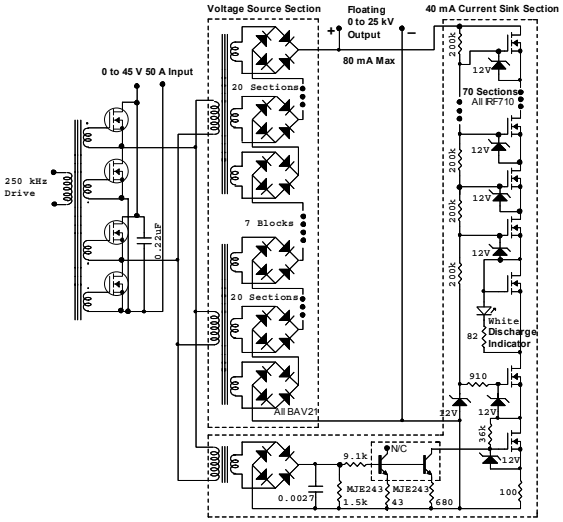

Fig.2. Simplified schematic of high-speed 25 kV converter.

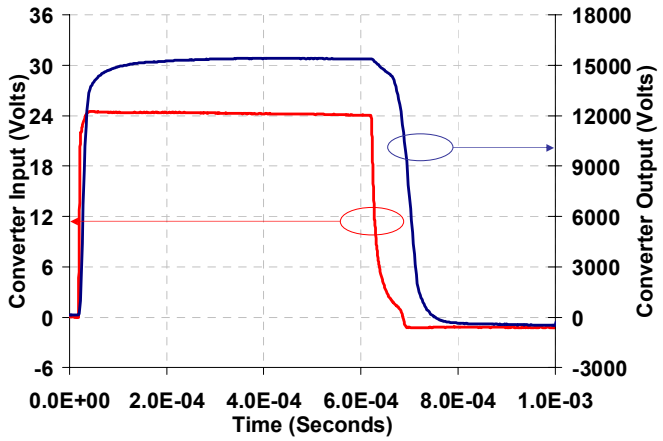

Fig. 3. Converter output vs. converter input.

inside of the safety-interlocked box. Another set of configuration jumpers located within the switching module of fig.1 are used to change between inductive and resistive load switching. For inductive switching, the oil capacitors work with the diode to perform clamped measurements. An external low-voltage supply (0 - 400 V) is used to charge the inductor. The inductor is reconfigurable and made up of four 480 µH, 25 A, low capacitance ferrite-core inductors. These can be placed in various series and parallel combinations with jumpers to obtain up to 1.9 mH at 25 A or 120 µH at 100 A. For resistive switching measurements, the diode and load inductor are changed to a plug-in load resistor. Drain voltage is measured with a 1000X probe and fed to one channel of an oscilloscope. Drain current is measured with a current transformer probe and fed to one channel of the scope.

Gate drive is provided using a low-inductance circuit based on a commercial gate-drive IC. The gate driver is driven with an external pulse generator at a low duty cycle, typically 0.1 %, to avoid DUT heating. The ground reference for the gate driver can be offset with an additional dc power supply if desired to provide a negative voltage in the off-state. Gate current is measured with a current transformer probe and fed to one channel of the scope. Gate voltage is also applied to one channel of the scope. Waveform data are collected from the four channels of the scope under the command of a LabView/CVI program.

For the inductors provided in the switching module of fig. 1, it is appropriate to use 100 µs pulses with a repetition rate of 0.1 s. The output of the pulse generator is used to trigger the scope, as well as provide the input to the gate driver IC. The external inductor charging power supply determines the DUT switching current; typically a hundred volts is needed for 10 A switching current with the 1.9 mH load. The clamping voltage is determined by the dc output voltage from the 750 watt power supply that is converted to high voltage by the 25 kV converter module.

C. 25 kV Converter

A simplified schematic of the 25 kV converter is shown in fig. 2. The converter contains a voltage-source section and a current-sink section. The voltage source section uses a MOSFET full-bridge modulator operating at 250 kHz. The modulator is based on a power modulation scheme for impedance conversion [5]. In this scheme, a source of low voltage at high current is transformed into a high voltage at low current by a ratio determined by transformers and series-connected rectified secondaries. For the voltage-source section of the 25 kV converter, seven transformers are used, and each transformer has 20 rectified secondaries, for a total of 140 stages. The primaries of the transformers are connected in parallel, and the turns ratio for primary to each secondary is 1:4. The large number of stages and low individual turns ratios allow the use of fast low voltage rectifiers and reduces transformer leakage inductance. These together provide much faster risetime than could be obtained by using a lesser number of stages and higher voltage transformation with each stage.

The voltage step-up ratio and current step-down ratio for the converter is 560, as determined by the transformer turns ratios and number of stages indicated above. The voltage risetime of this open-loop converter is limited mainly by the slew rate of the low-voltage, high-current driving source and the inductance of the cabling between this driving source and the converter. Using the 30 V, 25 A amplifier described above, the observed risetime for the 25 kV amplifier without load is 30 µs. This circuit is enabled only when the safety interlock switches are closed. The source section is thermally protected.

The current-sink section provides faster fall times than could be reasonably provided by bleeder resistors, especially if a dc storage capacitor is used for switching measurements. The current sink uses 70 series-connected MOSFET stages that can sink up to 40 mA. A driving transformer and contour circuit allow the full 40 mA sink capability only when the voltage-source section (see fig. 2) has zero output. The current sink current is reduced as the output from the voltage-source section increases. This circuit is designed to be fail safe in that, if power is lost, the current sink section will remain active to discharge the capacitors used for the switching measurements.

Fig. 3 shows the no load converter output in response to a 600 µs input pulse. The input pulse is obtained from a simple low on-resistance MOSFET source follower driven with a pulse generator. This is used for demonstrating the converter risetime because the source follower offers a faster risetime than the 30 µs risetime of the 750 watt amplifier/power supply. The 750 watt supply is used with a bypass capacitor to supply drain voltage for the MOSFET. The converter risetime is less than 20 µs, and the 24 V input is transformed to about 15 kV output.

Upon termination of the input pulse to the MOSFET source follower, the source voltage does not fall all the way to zero immediately, and as a result it is possible to observe the action of the current sink section of the converter. At the point where the input to the converter falls initially, the converter output begins to fall slowly (from 16 kV to 14 kV in fig. 3). During this time, the input to the converter is not low enough to cause the pull-down current-sink section of the converter to become active. The slow drop in output voltage is caused by the bleeder resistors that also serve as MOSFET series string biasing in the current-sink section. When the input to the converter falls to a low enough voltage, near zero, the current-sink section becomes active and the output voltage falls rapidly (from 14 kV to 0 V).

D. 20 kV Isolated Temperature-Controlled Heatsink

Accurate characterization of SiC devices requires that the measurements be made under controlled temperature conditions. Many of the devices tested do not have their own electrical isolation and, as a result, require an electrically isolated heatsink that can withstand the full voltages experienced by the DUT. Furthermore, it is common to see 50 ns switching rise and fall times at test voltages approaching 10 kV for current research devices, and these voltage transitions are applied directly to the temperature-controlled heatsink. Leakage measurements on these devices are currently performed up to 14 kV for this research effort and are expected to go higher. Temperature control of the heatsink requires the ability to both measure the temperature of the heatsink and to apply heating or cooling to obtain the desired temperature under feedback control. In the system described herein, heating is the method used to vary the temperature as measurements are done under short duty cycle pulsed conditions and forced air cooling is only used to reduce the heatsink temperature after high temperature measurements have been made. Both the temperature measurement and the heating power application must be performed with high-voltage isolation. Furthermore, it is of extreme importance to minimize the parasitic capacitances across these interfaces as capacitance limits DUT voltage risetime and any capacitive currents across the heating/measuring interface cause major noise/interference problems.

A block diagram of the DUT temperature-controlled heatsink system is given in Fig. 4. Magnetic coupling is used for both the temperature measurement interface and the heating power interface. For the temperature measurement, a 100 kHz current source is applied to the primary of a 1:1 toroidal transformer. A 100 ohm platinum RTD resistor is connected to the secondary of the transformer and installed in the heatsink. The resistor is operated at approximately 100 mV to avoid self heating. The resistance of the RTD is reflected through the transformer and coupled to a tuned amplifier and detector. After some linearization and ambient temperature compensation, the resultant dc voltage is applied to a commercial temperature controller configured for a linear input.

Another 1:1 toroidal transformer is used for the application of heating power to the heatsink. The primary of this transformer is driven from a full bridge square-wave converter operated at 50 kHz. The input power to the converter is taken from the output of an external 100 V heater supply amplifier driven in turn by the temperature controller to complete the feedback loop. The secondary of this transformer is connected to a heating resistor element installed in the heatsink. Since the temperature sensor voltage is much lower than the heating power voltage, care is required to avoid the temperature measurement being influenced by the heating power. The frequencies of the temperature sensing and the power delivery were chosen so that the 100 kHz tuned amplifier could reject the

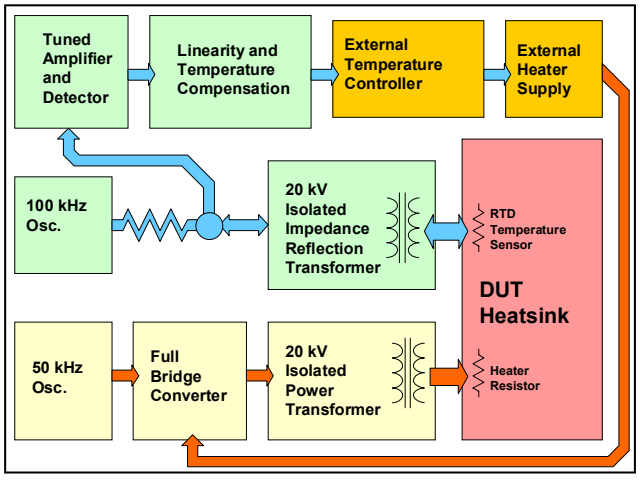

Fig. 4. Block diagram of isolated heatsink system.

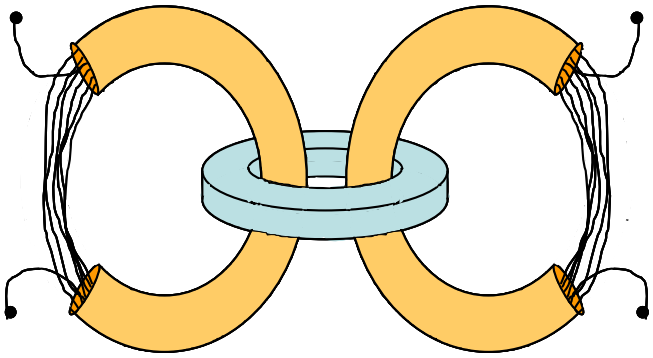

Fig. 5. Low-capacitance, high-voltage transformer construction for temperature-controlled heatsink.

fundamental power frequency of 50 kHz and its odd harmonics with maximum effectiveness.

Initially, these transformers were both wound with double-insulated wire on toroids for both primaries and secondaries. This construction produced too much parasitic capacitance between the primaries and the secondaries, and better designs were required. In order to minimize the parasitic capacitances, the transformer construction shown in fig. 5 is adopted. In this construction, insulated wire is threaded multiple times through insulating tubing for a given transformer winding. Both the primaries and the secondaries are constructed the same way, and each of the transformers has a 1:1 turns ratio. The tubing keeps the individual bundles of wire together and thus minimizes the capacitive coupling between the primary and secondary windings. For the temperature measurement transformer, each winding consists of 20 turns of # 30 AWG wire-wrap wire in a PVC tube using a TX22/14/6.4-3E25 core. For the heater power transformer six of these tubes bundled together were used, each containing five turns of # 26 AWG hook-up wire for a total of 30 turns, for each winding. A TX36/23/15-3E27 core is used for this transformer.

While the parasitic capacitance between the windings is very low with the construction shown in fig. 5, leakage inductance and susceptibility to external coupling is high. In order for the power transformer to have minimal effect on the temperature measurement transformer, the two transformers are carefully positioned orthogonal to one another. Additionally, the tubes containing the windings are pressed together and secured with shrink tubing so as to reduce the cross sectional area of the windings.

III. CURVE TRACER EMULATION SOFTWARE

The application software for the I-V parametric data acquisition of DUT characteristics is described in this section. The main goal of this application is to control a group of GPIB-interconnected instruments which collectively give the SiC DUT the required voltages and currents to stimulate and measure the response. Tests of interest usually include drain leakage, gate leakage, and transfer characteristics.

Fig. 6 shows the main panel user interface for the curve tracer. In addition to the main panel user interface, there are pop-up panels that are used to control specific functions in more detail. In fig. 6, three graph areas can be seen. The plots for these graphs are generated from two general processes. The first one occurs when the application controls the instruments needed to generate the required voltages and currents to be applied to the DUT and for the oscilloscope to acquire the DUT response and send the real-time captured waveforms back to the application. Two voltage waveforms are captured; one representing applied voltage and one representing response current. These two waveforms become the device voltage and current versus time once the application performs the required scaling as outlined in section II *A*. The resultant DUT voltage waveform is shown in the plot located in the upper right-hand corner of the user interface, and likewise the current waveform is displayed in the lower right-hand corner.

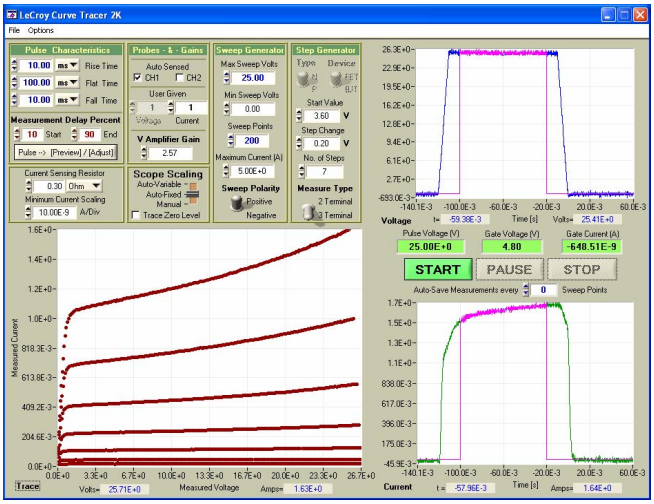

Fig. 6. Curve tracer virtual instrument user interface.

The second process consists of taking these two signals and generating the required display graph that shows the behavior of the DUT as it responds to applied voltages. This graph is a plot of voltage vs. current, thus eliminating time, and appears in the lower left-hand area of the user interface panel. This graph can show a single curve of current vs. voltage such as might be obtained from a leakage measurement or a set of parametric I-V curves for a MOSFET with different gate voltages. This latter case is an example of a three-terminal measurement and is represented in fig. 6.

To eliminate time for the generation of I-V plots, an averaging interval is applied to both the voltage and current waveforms. The waveform instantaneous values within the averaging interval are averaged to obtain a single value for

both voltage and current and these single current and voltage values are used to generate the individual points on the DUT I-V curves. The averaging interval limits are user definable and are shown as vertical lines on the voltage vs. time and current vs. time displays.

The two plots on the right-hand side of the interface are updated and displayed with each data point accumulated for the I-V parametric graph as the application runs. This process allows the user to make sure that the averaging interval is set appropriately and also to see other issues that affect the measurement. For example, it is apparent that the current shown in the lower right-hand plot in fig. 6 is rising with time. While it is the average of this current bracketed by the averaging interval that is used in the parametric graph, the time-dependent increase of current is evidence of DUT heating. The heating lowers the MOSFET threshold voltage and thus turns the device on progressively harder during the interval of the pulse. The observation of current is particularly useful when doing leakage and breakdown measurements of SiC devices because erratic behavior can be caused by various phenomena and the current signature can be useful in determining the failure mechanisms.

Various set-up features of the curve tracer are given in the following paragraphs. These features fall into groups that are directed at particular GPIB instruments in the total set-up of the test bed. The basic DUT driving pulse has a set of parameters that are used to set up an arbitrary waveform generator (AWG) that in turn drives the 750 watt amplifier/power supply. The step generator parameters are used to control a bipolar power supply for the gate/base drive for the DUT. The sweep generator parameters and amplifier gain are used to control pulse amplitude of the AWG. The probe gain parameters are used with the oscilloscope to specify the correct measurement scaling. An additional feature allows the user to save all, some, or none of the voltage and current waveforms for a particular set of parametric I-V curves.

Fig. 7 shows in detail the portion of the main user interface panel that is used to control most of the parameters. The *Pulse Characteristics* section is used to set pulse rise, duration, and fall time. The *Measurement Delay Percent* is used to control the averaging interval that is displayed on the voltage and current plots. The *Pulse Preview Adjust* activates a pull-down panel that is shown in fig. 8. Using the panel of fig. 8, the pulse rise and and/or fall can be softened as shown, and the measurement duty cycle can be reduced to minimize DUT heating.

Returning to fig. 7, the user-specified *Max Sweep Volts* associated with the *Sweep Generator* section is combined with the user-specified *V Amplifier Gain* to allow the application to calculate the correct pulse amplitude values needed from the AWG to obtain the desired voltage values that can ultimately be applied to the DUT through R_{LOAD} in the test bed. The application uses the *Minimum Sweep Volts*

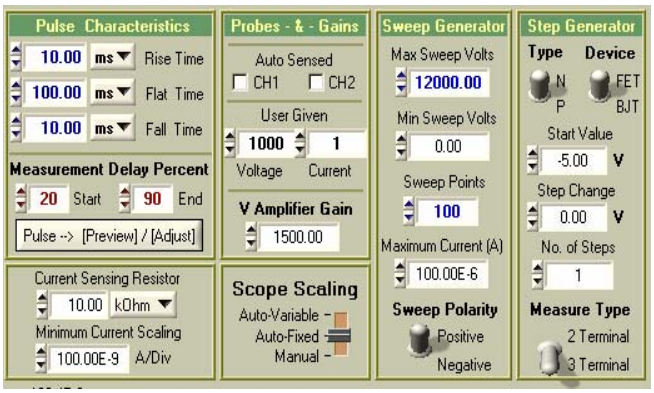

Fig. 7. Basic parameter adjustment area of main user interface.

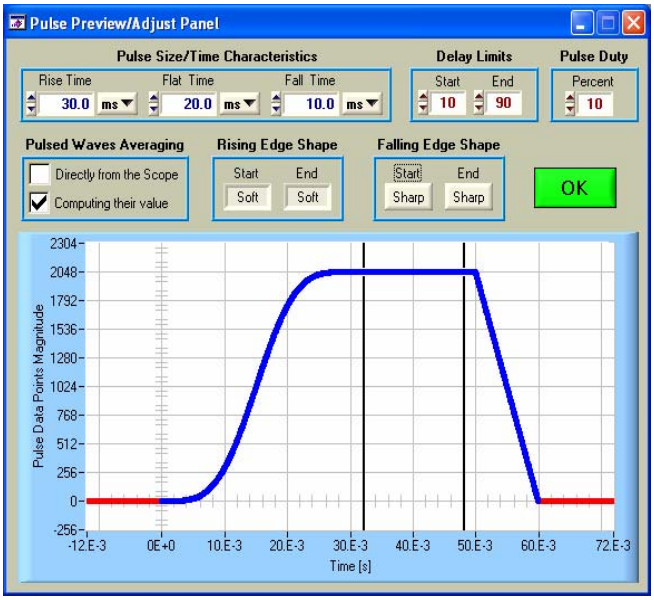

Fig. 8. Pulse adjustment sub panel.

and the *Sweep Points* to partition the sweep range into equal voltage steps.

The *Maximum Current* allows the user to specify the maximum current that the DUT is allowed to conduct before the application terminates the measurement. To avoid damage to the DUT, the user can specify a certain *Maximum Current* limit that can be checked during the measurement process. The measurements will continue as long as the DUT current does not exceed this limit. Once started, the measurement process will be finished only when all the sweep points are done, the current limit is exceeded, or the user manually interrupts the process, whatever occurs first.

The *Step Generator* is used to set up the voltage or current steps that are applied to the gate of the DUT for 3-terminal measurements. The polarity and device type can be selected, where the *FET* position results in a voltage drive and the *BJT* position results in a current drive to the DUT. The starting point, step amplitude, and number of steps can be selected.

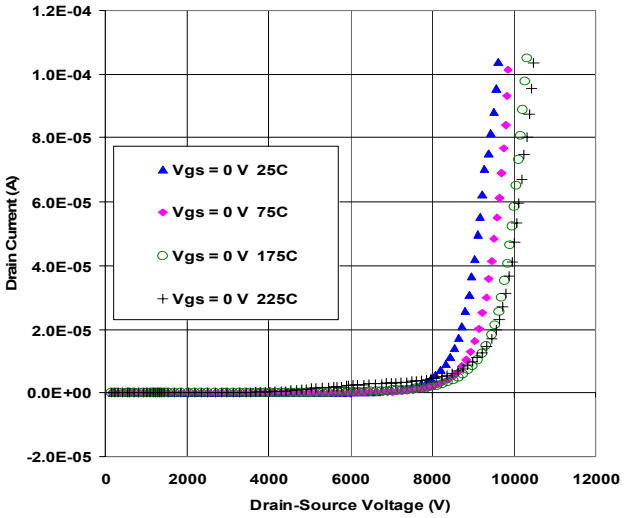

Fig. 9. Leakage current for a 10 kV SiC MOSFET area 0.125 cm^2 at various temperatures.

Several methods are available to the user to set up the scale sensitivity on the oscilloscope for the measurements. The *Scope Scaling* switch can be set in the *Manual* position whereby the user sets the scope sensitivity from the scope, and it remains at that setting for the duration of the measurement. The *Auto-Fixed* and *Auto-Variable* positions cause the scope sensitivities to be changed during the measurement to optimize the sensitivity settings for a given signal level. The auto scaling is done based on the amplitude of the waveform; if the waveform goes off-scale, the gain is reduced and the same pulse amplitude is repeated. If the waveform amplitude is too low, the gain is increased and the pulse is repeated. The *Auto-Fixed* position uses the standard scope 1-2-5 gain sequence and the *Auto-Variable* position allows fine gain adjustment. The auto-scaling functions slow the measurement since some pulses have to be repeated, but this method provides a higher dynamic range measurement which is particularly useful for leakage tests.

IV. Results and Discussion

This section shows some sample measurements of SiC devices that are being developed under a multi-phase Defense Advanced Research Projects Agency (DARPA) program. Some of this work is highlighted [6, 7]. Fig. 9 shows the leakage of a 10 kV SiC MOSFET with area 0.125 cm^2 rated at 5 A at various temperatures. The gate voltage for all temperatures is 0 V. The measurements shown are made at progressively higher temperatures. The breakdown voltage increases with increased temperature, consistent with an avalanche type of breakdown. Additional measurements on this device, not shown, indicate complete channel cutoff for a gate voltage of 1 V at 125 °C, but not complete cutoff at a gate voltage of 2 V at 25 °C.

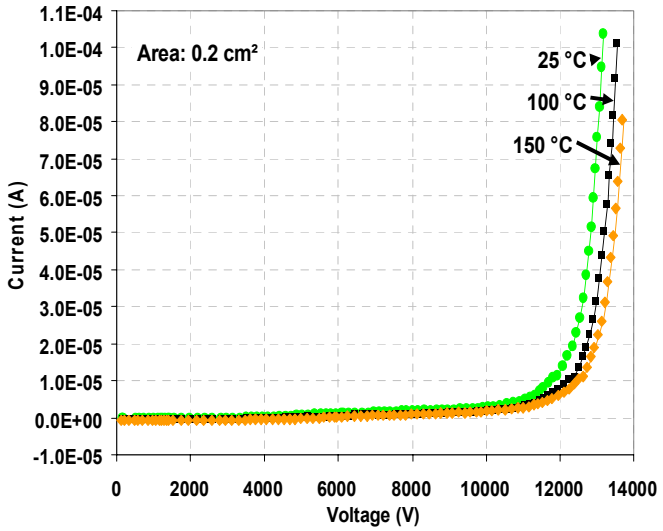

Fig. 10a. Leakage current for a 10 kV, 5 A SiC diode at various temperatures, linear scale.

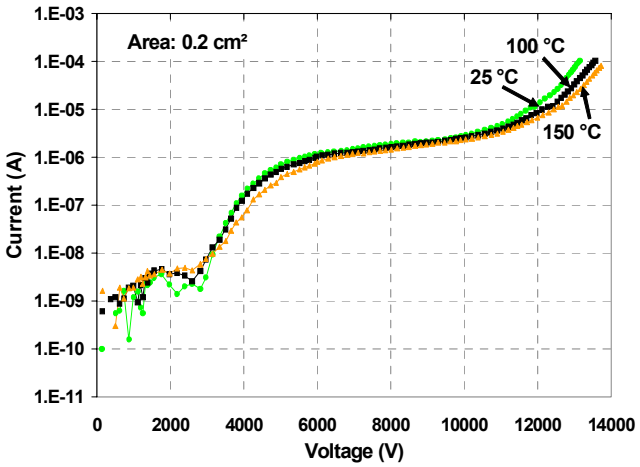

Fig. 10b. Same data as shown in fig. 10a but on a log current scale.

Fig. 10a shows leakage for a 10 kV, 5 A, 0.2 cm^2 diode at various temperatures, and fig. 10b shows the same data with a log current scale. The notable characteristic is that the breakdown voltage increases with increasing temperature. The log current scale plot demonstrates the dynamic range of the measurement that is taken using the auto-scaling feature of the curve tracer.

Fig. 11 shows inductive turnoff waveforms for a SiC MOSFET similar to the one shown in fig. 9. The effective gate drive source impedance is 4 Ω, and drain voltage and drain current waveforms are shown for 2 A and 12 A current turnoff with the DUT mounted to the temperature-controlled heatsink, as well as these same currents with the DUT not attached to the heatsink and floating. In both cases, the duty

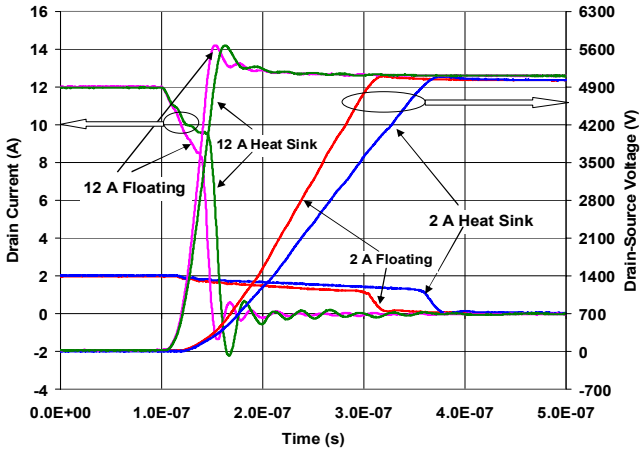

Fig. 11. Inductive load turnoff for a 10 kV SiC MOSFET area 0.125 cm^2. 2 A and 12 A current turnoff is shown both with the device mounted on the heatsink and with the device floating.

cycle is low and the temperature is at room temperature. The voltage clamp is set to 5 kV. Analysis of the differences in the voltage risetimes indicates that the parasitic capacitance at the drain terminal is about 60 pF, of which 39 pF is the DUT output capacitance and 21 pF is the capacitance of the isolated heatsink. The reductions in current from the initial values that occur during the voltage rise interval are caused by additional parasitic capacitance located on the clamping diode side of the current probe. This capacitance also includes that of the load inductor. By using the proportional drop in this current during the voltage risetime, this additional capacitance is observed to be about 14 pF. For this measurement, the four load inductors are configured in series.

V. Conclusion

A generalized 25 kV test bed developed to characterize high-voltage, high-power SiC devices is described. The test bed features containment of all high voltage circuits and the DUT within a clear plastic interlocked safety box. An open-loop power converter system provides up to 25 kV dc or 25 kV pulses with transitions as low as 30 µs. The output from the converter is used as the high voltage power supply for both pulsed curve tracer (parametric static measurements) and the continuous high voltage power supply required for inductive/resistive switching. The test bed includes user-configurable inductors, clamping capacitors, and high voltage resistive load modules for resistive and inductive load switching and an additional reconfigurable section for parametric device characterization. A flexible curve tracer computer user interface is used to define test parameters, to control instruments, and to process data. The DUT can be mounted on a 20 kV voltage-isolated temperature-controlled heatsink for temperature control up to 300 °C. The performance and parasitic elements of the test bed have been characterized using several example measurements of SiC devices.

References

[1]. R. Singh, K. G. Irvine, D. C. Capell, J. T. Richmond, D. Berning, A. R. Hefner, and J. W. Palmour, "Large Area, Ultra-high Voltage 4H-SiC p-i-n Rectifiers," IEEE Trans. on Electron Devices, Vol. 49, no. 12, pp. 2308-2316, Dec. 2002.

[2]. S.H. Ryu, et al., "10 kV, 123 mΩ-cm2 4H-SiC Power DMOSFETs," IEEE Electron Device Letters, Vol. 25, No. 8, pp.556-558, Aug. 2004.

[3]. Electric Power Research Institute (EPRI), 3412 Hillview Avenue, Palo Alto, California 94304, http://www.epri.com

[4]. Defense Advanced Research Projects Agency (DARPA), Microelectronic Technology Office (MTO), Wide Bandgap Semiconductor Technology High Power Electronics Program (WBG-HPE), BAA#06-30, Wide Bandgap Semiconductor Technology High Power Electronics, http://www.darpa.mil/mto/solicitations/index.html

[5]. D. Berning, "Output Transformerless Amplifier Impedance Matching Apparatus," US Patent 5,612,646, March 1997.

[6]. http://powerelectronics.com/news/silicon-carbide-components/

[7]. J.C. Zolper, "Emerging Silicon Carbide Power Electronics Components," IEEE Applied Power Electronics Conference Proceedings, Austin, TX, March 2005.